Amyloid-β-(1-42) increases ryanodine receptor-3 expression and function in neurons of TgCRND8 mice

Supnet, Charlene; Grant, Jeffrey; Kong, Hong; Westaway, David; Mayne, Michael

Publisher's version / Version de l'éditeur:
http://dx.doi.org/10.1074/jbc.M606736200
The Journal of Biological Chemistry, 281, 50, pp. 38440-38447, 2006

THE JOURNAL OF BIOLOGICAL CHEMISTRY VOL. 281, NO. 50, pp. 38440–38447, December 15, 2006

Amyloid-β-(1–42) Increases Ryanodine Receptor-3 Expression and Function in Neurons of TgCRND8 Mice*

Received for publication, July 14, 2006, and in revised form, October 5, 2006 Published, JBC Papers in Press, October 18, 2006, DOI 10.1074/jbc.M606736200

Charlene Supnet[‡§], Jeff Grant[‡¶1], Hong Kong[‡], David Westaway[‖], and Michael Mayne[‡§¶2]**

*From the [‡]Institute for Nutrisciences and Health, National Research Council of Canada, Charlottetown, Prince Edward Island C1A 5T1, the [§]Department of Biomedical Sciences, Atlantic Veterinary College/University of Prince Edward Island, Charlottetown, Prince Edward Island C1A 4P3, the [¶]Department of Pharmacology and Therapeutics, University of Manitoba, Winnipeg, Manitoba R3E 0T6, [‖]Centre for Research in Neurodegenerative Disease, University of Toronto, Toronto, Ontario M5S 3H2, and **Division of Neurodegenerative Disorders, St. Boniface General Hospital Research Centre, University of Manitoba, Winnipeg, Manitoba R2H 2A6, Canada*

Disruption of intracellular calcium homeostasis precedes the neurodegeneration that occurs in Alzheimer disease (AD). Of the many neuronal calcium-regulating proteins, we focused on endoplasmic reticulum (ER)-resident ryanodine receptors (RyRs) because they are increased in the hippocampus of mice expressing mutant presenilin-1 and are associated with neurotoxicity. Others have observed that ryanodine binding is elevated in human postmortem hippocampal regions suggesting that RyR(s) are involved in AD pathogenesis. Here we report that extracellular amyloid-β(Aβ)-(1–42) specifically increased RyR-3, but not RyR-1 or RyR-2, gene expression in cortical neurons from C57Bl6 mice. Furthermore, endogenously produced Aβ-(1–42) increased RyR-3 mRNA and protein in cortical neurons from transgenic (Tg)CRND8 mice, a mouse model of AD. Increased RyR-3 mRNA and protein was also observed in brain tissue from 4- to 4.5-month-old Tg animals compared with non-Tg littermate controls. In experiments performed in nominal extracellular calcium, neurons from Tg mice had significant increases in intracellular calcium following ryanodine or glutamate treatment compared with littermate controls, which was abolished by treatment with small interfering RNA directed to RyR-3, indicating that the higher levels of calcium originated from RyR-3-regulated stores. Taken together, these observations suggest that Aβ-(1–42)-mediated changes in intracellular calcium homeostasis is regulated in part through a direct increase of RyR-3 expression and function.

Alzheimer disease (AD)[3] is a neurodegenerative disorder characterized by neuritic plaques composed of aggregated extracellular amyloid-β (Aβ), intracellular neurofibrillary tangles, and containing selective neuron and synapse loss leading to irreversible cognitive decline and memory impairment (1). Although the cause of AD is still unknown, it is believed that accumulation of Aβ in the brain is an initial pathogenic event (2). Aβ-(1–42) is a fibrillogenic peptide resulting from the sequential endoproteolytic cleavage of amyloid precursor protein by β- and γ-secretase, and its overproduction and deposition are associated with early-onset (or familial) and sporadic AD (3). Consequently, there is an extensive effort to determine the molecular and cellular actions of Aβ on neurons and glial cells.

Alterations in intracellular calcium (Ca^{2+}_i) homeostasis constitute an early signaling event that initiates the manifestation of AD (4). Ca^{2+}_i levels are maintained by voltage-, ligand-gated, or store-operated Ca^{2+} channels on the plasmalemma and by endoplasmic reticulum (ER)-resident channels (5). Several studies have indicated that disruption of ER-regulated Ca^{2+}_i homeostasis is associated with neurotoxicity in AD (6). The ER is an important dynamic Ca^{2+} source and sink, it regulates neurotransmitter release, synaptic plasticity, gene expression, and signal transduction to the nucleus (7). Ryanodine receptors (RyRs) and inositol 1,4,5-trisphosphate receptors (IP_3Rs) are the two major Ca^{2+} release channels found on the ER (8) and are activated through Ca^{2+}-induced Ca^{2+} release and IP_3-induced Ca^{2+} release, respectively (9).

Our study focuses on the role of RyRs in the regulation of Ca^{2+}_i homeostasis because others have observed that hippocampal brain specimens from AD patients with early cognitive decline have increased ryanodine binding, suggestive of increased RyR levels (1). We observed that RyR expression and function were increased in neurons that expressed mutant PS-1 (10). Furthermore, high levels of RyRs mediated dysregulation of Ca^{2+}_i in cortical neurons from other mouse models of AD (11–13). In brain, RyRs are concentrated in postsynaptic neurons, astrocytes and oligodendrocytes, where they regulate Ca^{2+}_i levels, membrane potential, and second messenger systems. Three isoforms of RyRs have been identified as follows: type-1, which is found in skeletal muscle; type-2, which is concentrated in the heart; and type-3, which is concentrated in hippocampus (14), cerebral cortex, and corpus striatum (15). All isoforms exist in brain, where RyR-2 is the most abundant, but previous studies give no indication as to which isoform is

* This work was supported in part by the Manitoba Health Research Council, an industry award from the Alzheimer Society of Canada, Canadian Institute for Health Research, and AstraZeneca. The costs of publication of this article were defrayed in part by the payment of page charges. This article must therefore be hereby marked "*advertisement*" in accordance with 18 U.S.C. Section 1734 solely to indicate this fact.

[1] Supported by a graduate student fellowship from the Alzheimer Society of Canada.

[2] To whom correspondence should be addressed: Institute of Nutrisciences and Health, National Research Council of Canada, Rm. MO-02, 93 Mount Edward Rd., Charlottetown, Prince Edward Island C1A 5T1, Canada. Tel.: 902-566-7465; Fax: 902-569-4289; E-mail: michael.mayne@nrc.gc.ca.

[3] The abbreviations used are: AD, Alzheimer disease; ER, endoplasmic reticulum; RyR, ryanodine receptor; Ry, ryanodine; Tg, transgenic; RT, reverse transcription; ANOVA, analysis of variance; IP_3R, inositol 1,4,5-trisphosphate receptor; APP, amyloid precursor protein; CHAPS, 3-[(3-cholamidopropyl)dimethylammonio]-1-propanesulfonic acid; siRNA, small interfering RNA; LTP, long term potentiation; LTD, long term depression; AUC, area under the curve; Ca^{2+}_i, intracellular calcium; GSR, GeneSilencer reagent.

important in the dysregulation of $Ca^{2+}{}_i$ homeostasis in AD neurons.

The way Aβ regulates the expression and function of the machinery that mediates disruption of $Ca^{2+}{}_i$ homeostasis in AD remains unclear. Here we report that high levels of Aβ-(1–42) selectively elevated RyR-3 mRNA and protein levels *in vitro* and *in vivo*. Functionally, increased RyR-3 facilitated significant increases in $Ca^{2+}{}_i$ levels following ryanodine or glutamate treatment. These observations highlight a possible role for RyR-3 in the AD pathology.

EXPERIMENTAL PROCEDURES

Animals and Neuronal Cultures—APP695 (KM670/671NL+V717F) transgenic (Tg) CRND8 mice were a gift from Dr. David Westaway (University of Toronto) and have been described previously to exhibit Aβ plaques and cognitive defects by 3 months of age (16). Timed pregnant C57Bl6 mice were obtained from the animal housing facility at the University of Manitoba. Cerebral cortices were dissected from embryonic day 16 C57Bl6 or CRND8 (non-Tg or Tg) fetuses and used for primary culture of cortical neurons as described previously (10). CRND8 fetuses were genotyped for the APP695 double mutation by real time PCR (Platinum *Taq*DNA polymerase; Invitrogen) before cell dissociation and tissue pooling. The sequences of primers used for double mutant APP695 were as follows: 5′ TGT CCA AGA TGC AGC AGA ACG GCT ACG AAAA and 3′ AGA AAT GAA GAA ACG CCA AGC GCC GTG ACT. PCR products were generated by 30 cycles of 94/68/72 °C. PCR product levels were determined during each cycle by SYBR-Green I (1/10,000 dilution; Molecular Probes, Eugene, OR) using iCycler iQ real time PCR detection system (Bio-Rad). Non-Tg and TgCRND8 cortical tissues were pooled separately and seeded at 8×10^5 cells per well onto poly-D-lysine (Sigma)-coated 6-well culture plates, 6.5×10^5 cells per 40-mm glass coverslips for Ca^{2+} imaging experiments, or 8×10^5 cells per 25-mm glass coverslips for immunofluorescence assay. CRND8 cortical neurons were maintained as above. Experiments were performed on C57Bl6 primary cortical neurons following 8 days of *in vitro* culture. Experiments conducted on non-Tg or TgCRND8 cultures were completed following 5 days of *in vitro* culture to ensure high viability of Tg neurons. Cultures were ~80% MAP-2 (Chemicon, Sunnyville, CA)-positive neurons and 20% were glial fibrillary acidic protein (Abcam, Cambridge, MA)-positive astrocytes by immunofluorescence assay (data not shown).

Aβ Treatments of Primary Cortical Neurons—Aβ-(25–35), Aβ-(35-25), Aβ-(1–40), Aβ-(1–42), and Aβ-(42-1) peptides (Bachem, Torrance, CA) were prepared as 200 μM stocks in Locke's buffer containing 154 mM NaCl, 3.6 mM $NaHCO_3$, 5.6 mM KCl, 1.0 mM $MgCl_2$, 5 mM glucose, 5 mM HEPES, and 2.3 mM $CaCl_2$ (Fisher), pH 7.2, and incubated at 37 °C (5% CO_2 atmosphere) 24 h prior to use. C57Bl6 neurons were incubated with 1000 nM of Aβ-(25–35), Aβ-(35-25), Aβ-(1–40), Aβ-(1–42), or Aβ-(42-1) peptide for 18 h or with 100 or 1000 nM ionomycin (Sigma) for 30 min in conditioned media. Non-Tg and TgCRND8 primary cortical neurons were incubated with 1000 nM of Aβ-(1–40), Aβ-(1–42), and Aβ-(42-1), peptide or 1.3 μg/ml Aβ-(1–42) antibody (rabbit polyclonal IgG) (BIOSOURCE) or as a negative control 1.3 μg/ml gp-116 (HHV-6) antibody (mouse monoclonal IgG) (Advanced Biotechnologies, Inc., Columbia, MD) for 18 h.

Reverse Transcription-PCR—Total RNA was purified from 8×10^5 neurons or a small cortical section of the right hemisphere of the brain (~10 mg) from non-Tg and TgCRND8 mice using the GenElute Total Mammalian RNA isolation kit (Sigma). RT-PCR amplification of RyR-1 and RyR-3 mRNA was conducted as outlined previously (10). PCR amplification of RyR-2 mRNA was conducted using primers 5′ GAA TCA GTG AGT TAC TGG GCA TGG and 3′ CTG GTC TCT GAG TTC TCC AAA AGC, yielding a product of 650 bp. RyR-2 PCR products were generated by 35 cycles of 94/53/72 °C. IP_3R-1 levels were determined using 5′ TCA TGG AAA GCA GAC ACG AT and 3′ CCG CTC TGT GGT GTA ATA TA yielding a PCR product of 404 bp, generated by 30 cycles of 94/54/72 °C. SERCA-2b levels were determined using 5′ GGG AGT GGG GCA GTG GCA GC and 3′ CGT CTC TCT GGG CTG AGG GG yielding a PCR product of 350 bp, generated by 30 cycles of 94/62/72 °C. β-Actin levels were determined using 5′ ATG GAT GAC GAT ATC GCT GC and 3′ CGT ACA TGG CTG GGG TGT TG primers that yielded a PCR product of 399 bp, generated by 25 cycles of 94/53/72 °C. Alignment analysis of each primer was conducted to ensure that they were gene- and isoform-specific. Densitometric analysis of RT-PCR products was performed using NIH Image software, version 1.60. RyR pixel density levels were normalized to β-actin levels and are depicted as fold changes, where the untreated condition is considered 1-fold.

Western Blot Analysis—Non-Tg and TgCRND8 brains were harvested from 4- to 4.5-month-old mice (16–18 weeks) sacrificed by intraperitoneal injection of 50 mg/kg pentobarbital (Bimeda-MTC Animal Health Inc., Cambridge, Ontario, Canada) followed by decapitation. Whole brains were dissected on ice into cerebellar, cortical, hippocampal, and basal regions (the remainder of tissue after the removal of the cortex, hippocampus, and brain stem). Tissue was immediately homogenized on ice with 400 μl of lysis buffer containing 25 mM Tris, 50 mM HEPES, pH 7.4, 137 mM NaCl, 1% CHAPS, 2.5 mM dithiothreitol (Fisher) and protease inhibitor mixture (Roche Applied Science). Samples were incubated on ice for 1 h and then centrifuged at 950 × *g* to pellet insoluble proteins. 125 μg of supernatant was loaded onto a 3–8% Tris acetate NuPAGE® gradient gel (Invitrogen) and transferred under reducing conditions onto 0.4 μm polyvinylidene difluoride membranes (Fisher) on ice for 24 h at 20 V. Membranes were blocked with 5% nonfat milk in TBS for 1 h at room temperature and incubated in blocking buffer with 1/1000 dilution of RyR-1, -2, or -3 antibodies overnight at 4 °C (isoform-specific RyR rabbit polyclonal antibodies were a gift from Dr. V. Sorrentino, University of Siena, Italy). The same membranes were probed for actin (Santa Cruz Biotechnology, Santa Cruz, CA). RyR pixel density levels were normalized to actin levels and are depicted as fold changes, where the untreated condition is considered 1-fold.

Immunofluorescence Analysis—Non-TgCRND8 neurons seeded at 8×10^5 on poly-D-lysine-coated glass coverslips were treated with 1000 nM Aβ-(1–42) for 24 h on *in vitro* day 4 to elevate RyR expression. Non-Tg and TgCRND8 cultures were

fixed with 4% paraformaldehyde (Fisher) in phosphate-buffered saline (Sigma) on *in vitro* day 5 at 37 °C, 5% CO_2 for 12 min and permeabilized with HEPES/Triton buffer containing 20 mM HEPES, 300 mM sucrose, 50 mM NaCl, 3 mM $MgCl_2$, and 0.5% Triton X-100 (Fisher) for 10 min at room temperature. Cells were blocked with 5% goat serum (Sigma) in phosphate-buffered saline for 1 h at room temperature and incubated with 1/1000 dilution of RyR-1, -2, and -3 antibodies (17) in blocking buffer overnight at 4 °C. Neurons were incubated for 1 h at room temperature with secondary antibodies at 1/1000 dilution (Molecular Probes), and nuclei were stained using Hoechst 33342 (Sigma). Neurons were imaged using an Axioskop 2 *plus* (Carl Zeiss Canada, Ltd.) with Axiovision Release 4.2 software. For detection of RyRs, all images were exposed for 260 ms under fluorescein isothiocyanate.

Small Interfering RNA (siRNA) Design and Delivery—siRNAs were generated using the Dicer siRNA generation kit (Genelantis, San Diego) and were based on the rabbit RyR-3 mRNA sequence (GenBank™ accession number X68650). The region of the RyR-3 mRNA chosen showed 88% alignment with mouse RyR-3, 9.6% with mouse RyR-2, and 0% with mouse RyR-1 after BLAST analysis. Primers used to amplify RyR-3 from plasmid for diced siRNA generation were specific to mouse and rabbit RyR-3 as determined by alignment analysis. Tg neurons seeded at 8×10^5 per well in 6-well plates were transfected with 200 ng of siRyR-3 or nonspecific control siRNA (Qiagen, Mississauga, Ontario, Canada) using 3 μl of GeneSilencer® siRNA transfection reagent (Genelantis) per ml of conditioned media for 24 h. Gene silencing was confirmed 72 h post-transfection by RT-PCR and Western blot analysis as described previously. Transfection efficiency was determined using 1 μg of AlexaFluor 546®-labeled nonspecific siRNA (Qiagen) and calculated as the number of nuclei localized with siRNA ÷ total number of nuclei × 100%.

Measurement of Free Intracellular Calcium—Free intracellular Ca^{2+} ($Ca^{2+}{}_i$) levels were quantified using fluorescence ratio microscopy as described elsewhere (10), using the Ca^{2+} indicator dye Fura-2 (Molecular Probes). Fura-2 bound to Ca^{2+}, an indication of free Ca^{2+} levels, and was excited at 340 nm, and unbound Fura-2 was excited at 380 nm. $Ca^{2+}{}_i$ levels are depicted as a ratio of 340/380 nm emission at 510 nm. Briefly, 6×10^5 cells were loaded for 30 min with 1 μg/ml of acetoxymethyl ester (AM) Fura-2 in Locke's buffer. Cells were imaged on an inverted Zeiss microscope using a CoolSnapHQ (Roper Scientific Inc., Trenton, NJ) camera with a 40× oil objective lens. Changes in $Ca^{2+}{}_i$ levels were determined using Stallion Imaging software (Downingtown, PA). L-(+)-glutamic acid (EM Science, Gibbstown, NJ) was converted to 1 M stock of glutamate by addition of 10 N NaOH (Fisher) to pH 7.2. Ryanodine (Sigma) was prepared as a stock solution of 50 mM in 100% Me_2SO (Sigma). Treatments were delivered to neurons by perfusion. Experiments were performed in nominal extracellular Ca^{2+} (Locke's buffer without $CaCl_2$). Each experiment was repeated at least three separate times, 15–30 cells imaged at each time. Of the cells imaged, data were pooled from cells that responded to both glutamate and ryanodine.

Statistical Analysis—Densitometric analysis was performed using NIH Scion Image software, version 1.60. Data were analyzed using GraphPad Prism, version 3.02 (San Diego, CA). One-way ANOVA with Student-Newman-Keuls post-test was performed to determine the difference between means after treatment. Two-way ANOVA with Bonferroni post-test was used to determine the difference between genotypes and treatments and the possible interactions of each. Differences were considered significant at $p < 0.05$.

RESULTS

Aβ-induced RyR-3 mRNA Expression in Primary Cortical Neurons—To test the hypothesis that Aβ directly increased RyR mRNA levels, C57Bl6 cortical neurons were treated with Aβ-(1–42) peptide (1000 nM) for 18 h and analyzed for RyR mRNA levels (Fig. 1*A*). As determined by RT-PCR, C57Bl6 primary cortical cells incubated with 1000 nM Aβ-(1–42) increased RyR-3 mRNA levels 3.5 ± 1.38-fold S.E. ($n = 4$, $p < 0.001$, one-way ANOVA, Student-Newman-Keuls post-test). Although not statistically significant, RyR-1 mRNA increased ~2.4 ± 0.84-fold S.E. Treatment with Aβ-(25–35), Aβ-(35–25), Aβ-(1–40), and Aβ-(42-1) peptides did not alter RyR gene expression in primary cortical neurons from C57Bl6 (Fig. 1*A*). Furthermore, identical treatments did not alter RyR-2, IP_3R-1, or SERCA-2b mRNA levels (not shown). To rule out the involvement of rapid increases in $Ca^{2+}{}_i$ in the up-regulation of RyR gene expression, we treated C57Bl6 primary cortical neurons with an ionophore, ionomycin, for 30 min. The treatment was removed and replaced with conditioned media for 18 h at 37 °C. Consistent with the observations made in a previous study (18), we did not see an induction of RyR gene expression after treatment with ionomycin ($n = 2$). Cell viability was unaltered by a 30-min treatment with ionomycin as assessed 18 h after treatment by trypan blue exclusion assay (data not shown).

RyR-3 Transcription and Protein Levels Are Increased in TgCRND8 Mice—Because Aβ increased RyR gene expression in primary cortical neurons, we hypothesized that RyR-3 expression is elevated in TgCRND8 mice, a mouse model of Alzheimer disease that produces high levels of Aβ and expresses early cognitive decline (16). Examination of cerebrum (forebrain) from the right hemisphere of 4–4.5-month-old TgCRND8 animals showed that RyR-3 mRNA levels were ~2.6 ± 0.43-fold S.E. higher ($n = 16$, $p < 0.01$, two-way ANOVA, Bonferroni post-test) compared with their non-Tg littermates (Fig. 1*B*). There was no change in RyR-1 and RyR-2 (Fig. 1*B*) or in IP_3R-1 and SERCA-2b mRNA levels (not shown). To determine where in TgCRND8 brain the increases in RyR were located, lysates of different brain regions dissected from 4- to 4.5-month-old CRND8 mice were analyzed for RyR protein by Western blot analysis using isoform-specific antibodies (17). Similar to mRNA levels, RyR-3 levels were increased ~2.7 ± 0.42-fold S.E. ($n = 14$, $p < 0.001$, two-way ANOVA, Bonferroni post-test) in the cortex of Tg mice as compared with non-Tg, whereas RyR-1 and RyR-2 levels were unchanged (Fig. 1*C*). RyR-3 levels were increased 1.9 ± 0.26-fold S.E. in the hippocampus as well ($n = 14$, $p < 0.01$, two-way ANOVA, Bonferroni post-test) but were unchanged in the basal and cerebellar regions (Fig. 1*D*). Our statistical tests reveal that these differences in RyR-3 expression are attributed to the genotype ($p < 0.0001$) and specific to the brain region ($p = 0.0011$).

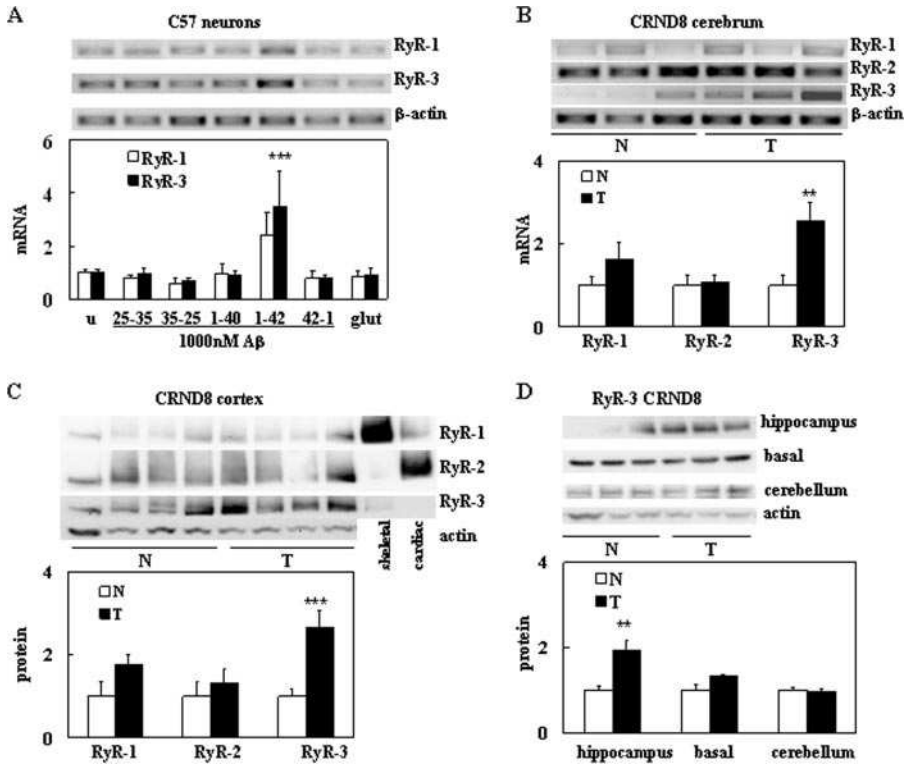

FIGURE 1. **RyR mRNA and protein are increased in the cerebrum of TgCRND8 mice.** *A,* representative agarose gel showing relative levels of RyR RT-PCR products from C57Bl6 cells. Neurons (*in vitro* culture day 8) were treated with 1000 nM of various Aβ peptide fragments for 18 h. Relative RyR-1 and RyR-3 RT-PCR products were normalized to β-actin levels. Neurons were treated with 20 μM glutamate (*glut*) as a stress response control. Values are the mean ± S.E. of fold change determinations made in samples from four cultures; ***, $p < 0.001$ compared with values for untreated (*u*) cells (one-way ANOVA with Student-Neuman-Keuls post-test). *B,* representative agarose gel showing levels of RyR-1, RyR-2, and RyR-3 RT-PCR products from 4- to 4.5-month-old CRND8 cerebrum. Non-Tg (*N*) are littermate controls, and TgCRND8 (*T*) are heterozygous for the APP695 double mutation. Values are the mean ± S.E. of the fold changes of RyR RT-PCR products from 16 mice each of non-Tg and TgCRND8. **, $p < 0.01$ compared with littermate control values (two-way ANOVA with Bonferroni post-test). *C,* representative immunoblot of RyR proteins from cortex of 4 non-Tg and 4 TgCRND8 mice at 4–4.5 months of age probed with anti-RyR-1, -2, and -3. Skeletal and cardiac muscle microsomes were used as positive controls for RyR-1 and RyR-2, respectively. Values are the mean ± S.E. of fold changes in RyR levels from four separate experiments (3–4 brains of non-Tg and TgCRND8 were used for each experiment, $n = 14$). ***, $p < 0.001$ compared with littermate control values (two-way ANOVA with Bonferroni post-test). *D,* immunoblot of RyR-3 proteins from hippocampus, basal region, and cerebellum of three non-Tg and three TgCRND8 mice at 4–4.5 months of age. Values are the mean ± S.E. of fold changes in RyR levels from four separate experiments (3–4 brains of non-Tg and TgCRND8 were used for each experiment, $n = 14$). **, $p < 0.001$ compared with littermate control values (two-way ANOVA with Bonferroni post-test).

Aβ Increased RyR-3 mRNA and Protein Levels in CRND8 Cortical Neurons—Based on our observations that Aβ increased RyR gene transcription in naive cortical neurons (Fig. 1*A*) and that RyR levels are increased in TgCRND8 brain samples (Fig. 1, *B–D*), we hypothesized that the cortical neurons of TgCRND8 mice had increased RyR gene expression. Primary neuronal cultures from TgCRND8 animals had an increase of ~3.6 ± 0.71-fold S.E. ($n = 3$, $p < 0.001$, two-way ANOVA, Bonferroni post-test) in RyR-3 mRNA levels as determined by RT-PCR compared with non-Tg littermate controls on *in vitro* day 5 (Fig. 2*A*). Aβ-(1–42) treatment of non-TgCRND8 neurons increased gene expression of RyR-3 3.1 ± 0.17-fold S.E. compared with untreated ($n = 3$, $p < 0.001$, two-way ANOVA, Bonferroni post-test) to levels comparable with those expressed in TgCRND8 neurons (Fig. 2*A*). Other treatments, including Aβ-(1–40) and Aβ-(42-1), did not influence RyR-3 gene expression, nor did IP_3R-1 and SERCA-2b mRNA levels differ between non-Tg and TgCRND8 neurons (not shown). As an alternative approach to determine whether extracellular Aβ was directly involved in elevating RyR gene expression, we treated TgCRND8 neurons with Aβ-(1–42) antibody (1.3 μg/ml) for 18 h. Quenching of extracellular Aβ-(1–42) decreased neuronal RyR-3 mRNA levels in Tg neurons by 2.2 ± 0.30-fold S.E. compared with untreated ($n = 3$, $p < 0.001$, two-way ANOVA, Bonferroni post-test) to levels similar to non-TgCRND8 littermates (Fig. 2*B*). Our statistical tests reveal that these differences in RyR-3 expression are attributed to the genotype ($p < 0.0001$) and specific to the type of treatment ($p = 0.0056$). To determine relative RyR protein levels in CRND8 neurons, an immunofluorescence assay was performed with using isoform-specific RyR antibodies. RyR-3 levels were markedly increased in TgCRND8 primary cortical neurons compared with their non-Tg littermate control cultures (Fig. 2*C*), whereas RyR-1 and RyR-2 levels did not change. Similarly, non-Tg neurons treated with Aβ-(1–42) (1000 nM) for 18 h had increased RyR-3, but not RyR-1 or RyR-2, levels comparable with Tg neurons (Fig. 2*C*).

Targeting RyR-3 by Gene Silencing Techniques—It was reported recently that RyR levels are increased in other models of AD, and as a result neurons from transgenic mice have elevated responses to 20–25 mM caffeine (12, 13). Given our observations showing increased RyR-3 levels in TgCRND8 neurons, we wanted to determine whether RyR-3 was involved in the elevated response. Because of a lack of pharmacological tools to selectively block RyR-3, we opted for a molecular approach to target RyR-3 and depress its expression in Tg neurons prior to Ca^{2+} imaging studies. Diced siRNAs selective for RyR-3 were generated to span a 613-bp section of the mRNA and knock down RyR-3 levels. 200 ng of siRyR-3 was transfected into Tg neurons with GeneSilencer reagent (GSR) for 24 h. At 72 h post-transfection, RyR-3 levels were significantly decreased by 2.9 ± 0.47-fold S.E. compared with untreated ($n = 4$, $p < 0.001$, two-way ANOVA, Bonferroni post-test) and were comparable with non-Tg neurons (Fig. 3*A*), whereas RyR-1 and RyR-2 levels did not change (fold changes not shown). Tg neurons treated with GSR, siRyR-3 alone, nonspecific siRNA alone (200 ng), and siRNA with GSR did not show significant changes in RyR-1, -2 (not shown), or -3 (Fig. 3*A*) mRNA levels. To determine the transfection efficiency of

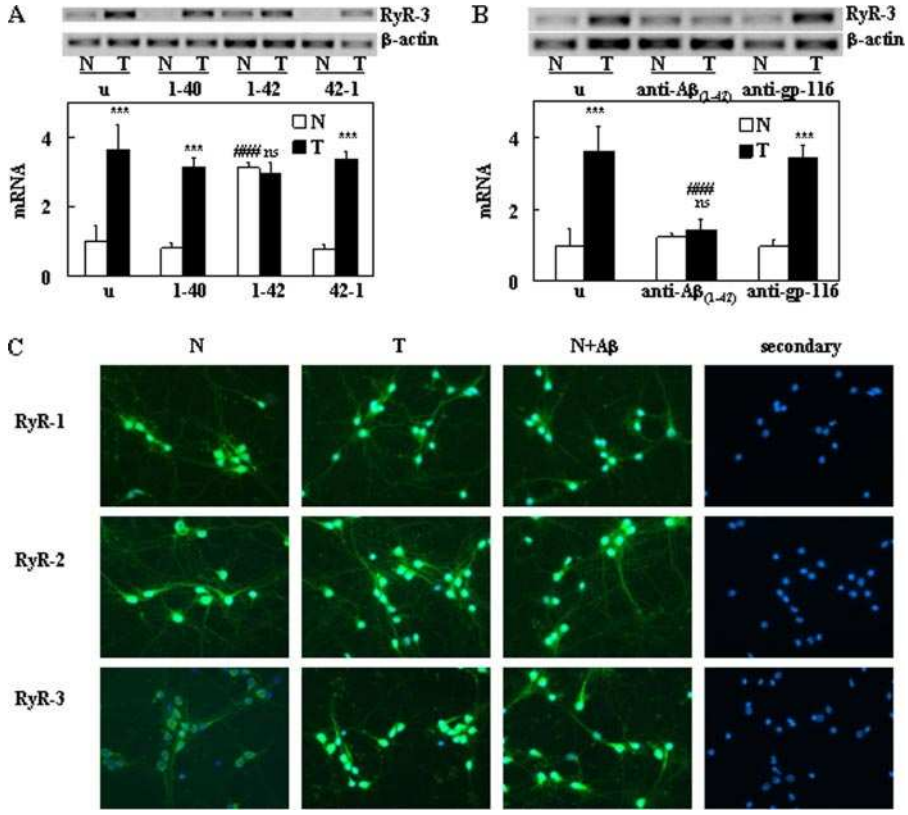

FIGURE 2. **Levels of RyR-3 are increased in cortical neurons of TgCRND8 mice.** *A,* representative agarose gel showing fold changes of RyR-3 RT-PCR products from embryonic day 16 CRND8 primary cortical neurons. Neurons cultured for 4 days were treated with 1000 nM Aβ peptides as before (Fig. 1*A*). Cells were collected on *in vitro* day 5. Non-Tg (*N*) are littermate controls, and Tg (*T*) neurons are heterozygous for the APP695 double mutation. Values are the mean ± S.E. of determinations made in samples from three cultures. Tg values were compared with littermate controls (non-Tg) at all treatments (*ns* indicates no statistical difference; ***, $p < 0.001$), and Aβ-treated non-Tg values were compared with untreated (*u*) non-Tg (###, $p < 0.001$, two-way ANOVA with Bonferroni post-test). *B,* representative agarose gel showing fold changes of RyR-3 RT-PCR products from 4-day-old cultures treated with 1.3 μg/ml Aβ-(1–42) antibody or 1.3 μg/ml gp-116 antibody (non-specific monoclonal antibody control) for 18 h at 37 °C before analysis (cells collected at *in vitro* day 5). Values are the mean ± S.E. of determinations made in samples from three cultures. Tg values were compared with littermate controls (non-Tg) at all treatments (*ns* indicates no statistical difference; ***, $p < 0.001$) and anti-Aβ-treated Tg values were compared with untreated Tg (###, $p < 0.001$, two-way ANOVA with Bonferroni post-test). *C,* immunofluorescence assay for RyR-1, RyR-2, and RyR-3 protein in non-Tg and Tg primary cortical neurons is representative of three separate cultures. Non-Tg neurons are treated with 1000 nM Aβ-(1–42) peptide as before (Fig. 1*A*). Cells were imaged at 400× magnification.

our experiments, we transfected Tg neurons with AlexaFluor 546®-labeled nonspecific siRNA (1 μg) under the same conditions as the siRyR-3 experiments. A transfection efficiency of 74.2 ± 8.3 S.E. % ($n = 4$ (12 separate fields total), $p < 0.001$, one-way ANOVA, Student-Newman-Keuls post-test) was obtained at 72 h post-transfection. Knockdown of RyR-3 protein levels in Tg neurons was confirmed by Western blot using isoform-specific antibodies ($n = 3$, Fig. 3*C*). At 72 h post-transfection, RyR-3 levels were reduced to 1.79-fold ± S.E. ($p < 0.05$, one-way ANOVA, Student-Newman-Keuls post-test) that of untreated Tg neurons. This is a reduction of 44.4 ± 4.5 S.E. %. RyR-1 and RyR-2 levels were unchanged after any treatment (fold changes not shown).

Calcium Released from ER Stores Is Increased in TgCRND8 Neurons Expressing Elevated Levels of RyR-3—To determine some of the functional consequences of increased levels of RyR-3 in TgCRND8 mice, we measured $Ca^{2+}{}_i$ levels of neurons after treatments of glutamate and ryanodine. Because of our interest in the contribution of ER Ca^{2+} stores to the overall $Ca^{2+}{}_i$ response, experiments were conducted in the presence of nominal extracellular Ca^{2+} to minimize the contribution of Ca^{2+} influx. Increased $Ca^{2+}{}_i$ because of glutamate is closely associated with neurotoxicity (19–23) and with alterations in AD neurophysiology (24); therefore, we sought to determine whether Tg neurons had altered $Ca^{2+}{}_i$ responses because of increased RyR-3. TgCRND8 neurons at *in vitro* day 5 demonstrated an elevated $Ca^{2+}{}_i$ response to 250 μM glutamate treatment as compared with non-Tg littermate controls (Fig. 4*A*), with a peak response of 0.67 ± 0.01 S.E. Fura-2 fluorescence ratio 340/380 nM ($n = 15$, $p < 0.001$, one-way ANOVA, Student-Newman-Keuls post-test) for Tg neurons was in contrast to 0.55 ± 0.03 S.E. 340/380 nM for non-Tg ($n = 18$) (Fig. 4*B*). To determine the contribution of RyR-3 to the observed increases in $Ca^{2+}{}_i$ levels, Tg neurons were treated with siRyR-3 for 72 h prior to Ca^{2+} imaging experiments. Knockdown of RyR-3 levels resulted in a decreased Ca^{2+} response of Tg neurons to glutamate (Fig. 4*A*), with a peak response of 0.52 ± 0.02 S.E. ratio 340/380 nM (Fig. 4*B*) that was significantly lower than non-Tg (0.55 ± 0.06 S.E., $n = 15$, $p < 0.05$, one-way ANOVA, Student-Newman-Keuls post-test).

To determine the direct contribution of RyR-gated Ca^{2+} stores to $Ca^{2+}{}_i$ levels, we performed experiments using an agonistic concentration (100 nM) of ryanodine (Ry) in the presence of nominal extracellular Ca^{2+}. After treatment of glutamate, ER stores become charged with Ca^{2+} and are then available for Ca^{2+} liberation (25). TgCRND8 neurons had increased $Ca^{2+}{}_i$ levels after 100 nM Ry treatment (Fig. 4*A*), with a peak response of 0.50 ± 0.01 S.E. ratio 340/380 nM ($n = 15$, $p < 0.001$, one-way ANOVA, Student-Newman-Keuls post-test) as compared with littermate controls (Fig. 4*C*). siRyR-3 treatment of Tg neurons prior to the experiment reduced the $Ca^{2+}{}_i$ response to Ry (Fig. 4*A*) to peak levels that were not significantly different from littermate controls (Fig. 4*C*).

To determine the role of ER Ca^{2+} load, we calculated the area under the curve (AUC) of our Fura-2 traces (Fig. 4, *D* and *E*). AUC calculations, or the ratio of 340/380 nM multiplied by time and depicted in arbitrary units, represent the total amount of Ca^{2+} being liberated from the ER after glutamate or Ry treatment. In both instances, Tg neurons had higher levels of ER Ca^{2+} released after agonist treatment ($n = 15$, $p < 0.01$, $p <$

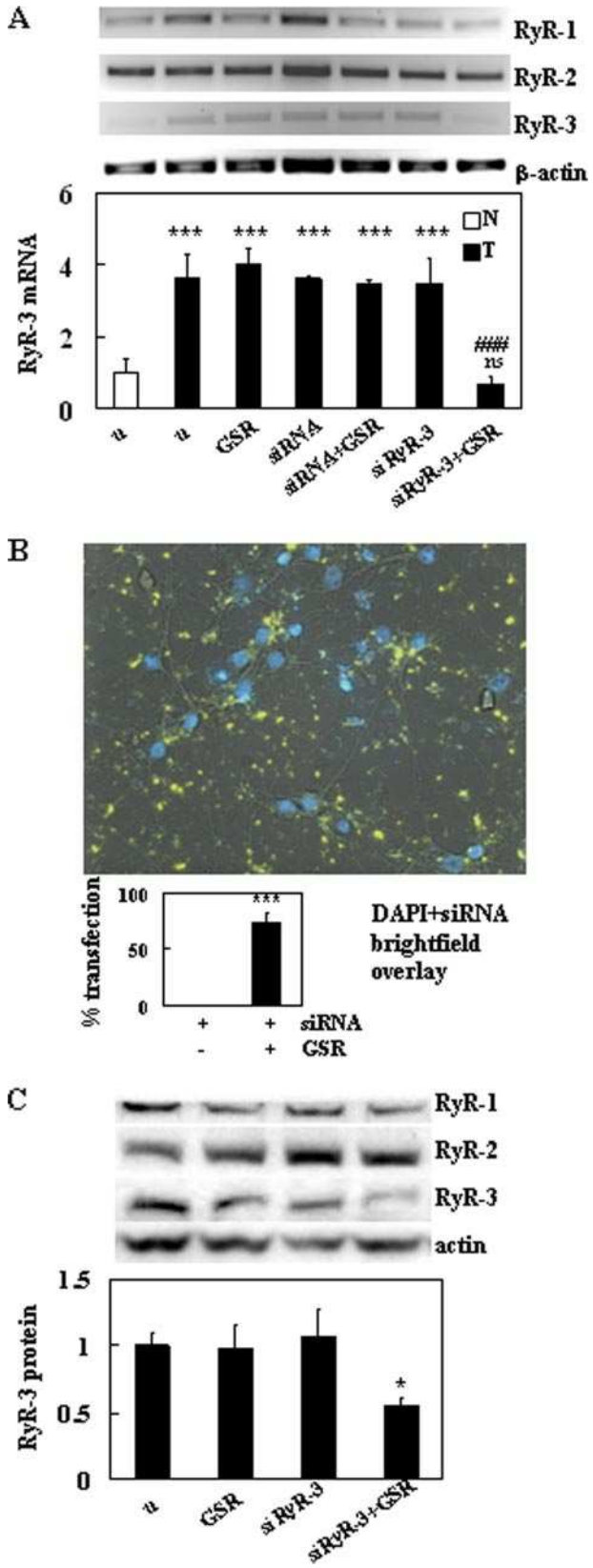

FIGURE 3. **Levels of RyR-3 mRNA and protein are decreased in TgCRND8 neurons after treatment with siRNA.** *A,* representative agarose gel showing fold changes of RyR-1, RyR-2, and RyR-3 RT-PCR products from non-Tg (*N*) and TgCRND8 (*T*) 8.0 × 10^5 primary cortical neurons treated with siRNA. RT-PCR analysis was conducted 72 h post-transfection. The treatments include untreated (*u*), 3 μl of GSR, 200 ng of control siRNA, or 200 ng of siRyR-3. The *graph* is representative of the relative expression of RyR-3. Values are the mean ± S.E. of the fold change of RyR-3 RT-PCR levels from four cultures each of non-Tg and Tg. Tg values were compared with untreated (*u*) littermate (non-Tg) at all treatments (*ns* indicates no statistical difference; ***, $p < 0.001$), and T+siRyR-3+GSR was compared with untreated Tg (###, $p < 0.001$, two-way ANOVA with Bonferroni post-test). *B,* image of Tg neurons transfected with 1 μg of AlexaFluor 546®-labeled nonspecific siRNA at 72 h post-transfection. Nuclei were labeled with Hoechst 33342 and imaged under 4′,6-diamidino-2-phenylindole (*DAPI*). The *graph* is representative of transfection efficiency of GSR and is pooled from three separate experiments. siRNA+GSR was ***, $p < 0.001$ (one-way ANOVA with Student-Newman-Keuls post-test) compared with siRNA treatment alone. *C,* representative immunoblot for RyR-1, RyR-2, and RyR-3 in Tg neurons treated with siRyR3 as in *A* and is representative of three separate cultures. The *graph* is representative of RyR-3 protein levels relative to actin, and values are the mean ± S.E. of the fold change of RyR-3. *, $p < 0.05$ (one-way ANOVA with Student-Newman-Keuls post-test) compared with untreated.

0.001, one-way ANOVA, Student-Newman-Keuls post-test) compared with littermate controls. After knockdown of RyR-3 levels by siRyR-3 treatment, Tg neurons had similar AUC values to non-Tg littermates.

DISCUSSION

Several studies now clearly implicate a role for RyRs in the development and progression of Alzheimer disease (10–13). Findings here have implicated RyR-3 as a key player in altering Ca^{2+} homeostasis of neurons in response to Aβ. We have come to this conclusion based on the following evidence. First, our *in vitro* studies show that Aβ-(1–42), regardless of the source of peptide (endogenously produced or synthetic), increased levels of RyR-3. As a direct consequence, Tg neurons had exaggerated $Ca^{2+}{}_i$ responses to ryanodine and to glutamate, which can trigger CICR from RyR stores (4, 26–29). Second, after knockdown of RyR-3 levels by siRNA, Ca^{2+} imaging experiments confirmed that the RyR-3 pools represented the majority of the glutamate-induced increase in Ca^{2+} in Tg neurons. Finally, RyR-3 levels were increased *in vivo* in the cortex and hippocampus, areas of the brain affected in AD, and suggest an important role for RyR-3 in disease progression.

It is well documented that alterations in Ca^{2+} homeostasis occur early in AD, before profound neuronal damage and cell death (4, 30). These changes in $Ca^{2+}{}_i$ levels appear to correlate more closely with cognitive decline compared with the formation of Aβ-containing senile plaques, the pathological hallmark of AD (31). It is interesting to note that TgCRND8 mice begin to display cognitive defects in spatial learning tasks at 19–22 weeks of age, where their ability to acquire new information is impaired (32). Of relevance to our study, we observed an increase in RyR-3 levels and Ca^{2+} disruption within this time frame.

The impact of dysregulated Ca^{2+} homeostasis as a result of increased RyR-3 in the in AD is still unclear. In fact, the exact function of RyR-3 in brain has yet to be determined, although their relative abundance in neurons of the hippocampus suggests a role for RyR-3 in hippocampal Ca^{2+} regulation (14). The generation of RyR-3 knock-out mice has given some insight into its function. Two independent groups have generated RyR-3 knock-out mice, and each group performed electrophysiological and behavioral studies to determine the role of RyR-3 in synaptic plasticity and hippocampus-dependent learning (33, 34). Both groups demonstrated evidence of increased long term potentiation (LTP), a physiological corre-

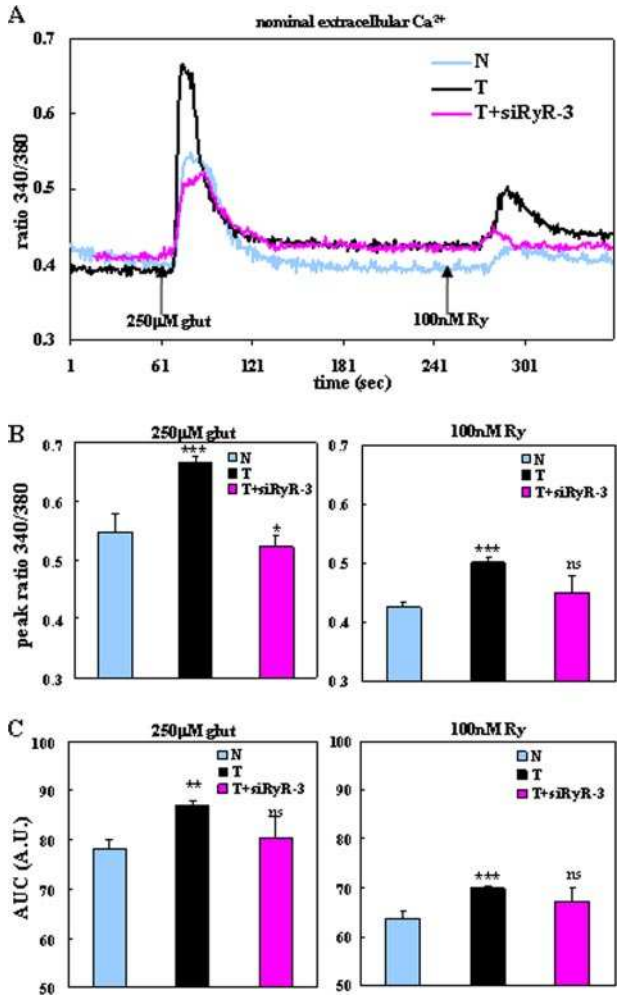

FIGURE 4. **Calcium release from ER stores was significantly enhanced in TgCRND8 primary cortical neurons via RyR-3 compared with littermate controls.** *A,* representative recording of the average changes in Fura-2 340/380 nm ratios of non-Tg (*N*), Tg (*T*), and T+siRyR-3 neurons in the presence of nominal extracellular calcium. The *arrows* represent the application of glutamate (*glut*) or ryanodine (*Ry*). The *traces* are representative of at least three separate experiments, $n = 15$ (*N*), $n = 18$ (*T*), and $n = 12$ (*T+siRyR-3*). *B, graphs* show the average peak response and S.E. of determinations made from at least three experiments. *ns* indicates no statistical significance; *, $p < 0.05$; ***, $p < 0.001$ compared with non-Tg (one-way ANOVA with Student-Neuman-Keuls post-test). *C, graphs* showing the AUC of the corresponding traces in *A*. *ns* indicates no statistical significance; **, $p < 0.01$; ***, $p < 0.001$ compared with non-Tg (one-way ANOVA with Student-Neuman-Keuls post-test). Basal ratios of neurons under the various conditions were not statistically different from each other.

late for learning and memory, after particular types of stimulation, namely short or weak tetanus, suggesting a role for RyR-3 in the depression of LTP and long term depression (LTD). However, after subjecting the RyR-3-deficient mice to the Morris water maze to assess spatial learning competencies, the two groups came to contradictory conclusions. Although Futatsugi *et al.* (34) showed that mutant mice had enhanced spatial learning, which would be expected if RyR-3 mediated the depression of LTP, Balschun *et al.* (33) observed that RyR-3 knock outs had significant deficiencies in their ability to acquire new information compared with mice with wild-type RyR. Interestingly, it has been shown that RyR-mediated Ca^{2+} release from post-synaptic CA1 (35, 36) or pre-synaptic CA3 (35, 37) neurons is required for the induction of LTD. Of the three different RyR isoforms, RyR-3 would be the likely candidate for the fine-tuning of these synaptic changes. RyR-3 is less sensitive to Ca^{2+} in comparison to RyR-1 and RyR-2 and therefore requires higher cytosolic Ca^{2+} levels to be activated and deactivated (38). Taken together, these observations suggest that RyR-3 may contribute to synaptic plasticity by modulating the balance between LTP and LTD, and the up-regulation of RyR-3 could be a response to an increase in neuronal excitability.

Such a mechanism could be at play in AD, and the up-regulation of RyR-3 might be an effort mounted by neurons to protect against the increased excitability brought about by the pathology of AD, specifically Aβ accumulation. Other aspects of $Ca^{2+}{}_i$ signaling in AD neurons are also enhanced, in particular *N*-methyl-D-aspartic acid receptor (39) and IP_3R-mediated signaling (40), leading to increased excitotoxicity. In fact, Stutzmann *et al.* (12) showed that RyR Ca^{2+} stores were directly responsible for the exaggerated hyperpolarization responses of PS1 mutant neurons to IP_3 and therefore impacted membrane excitability. Furthermore, RyR-3 mRNA was transiently increased in rat brain after kainic acid-induced status elipticus (41), implicating a role in modulating excitability. Higher levels of RyRs could be considered advantageous in protecting against putative excitotoxicity in AD, but the implications of chronic up-regulation of RyR-3, which could occur as long as Aβ is being produced, might lead to the opposite effect. As the balance of excitation and depression are skewed, the resulting effect could be an increase to overall $Ca^{2+}{}_i$ levels, oxidative stress, and activation of pathways leading to toxicity and neurodegeneration (10, 11, 41). Further studies are required to resolve why RyR-3 is being up-regulated so significantly and specifically in TgCRND8 mice.

The results of our study describe a mechanism by which Aβ contributes to the dysregulation of intraneuronal Ca^{2+} homeostasis by up-regulating the expression and function of a specific ER Ca^{2+} release channel, RyR-3. There is much evidence to suggest that RyR Ca^{2+} pools play an important role in the neuronal dysfunction initiated by Aβ deposition in AD (10–13). Our findings further focus on RyRs and implicate RyR-3 as the primary ER channel that facilitates Ca^{2+} disruption in AD. This information could be significant in understanding the neurobiology of AD pathology. RyR(s) may play a role in normal aging as well as contribute to AD pathology. In a report by Lu *et al.* (42), RyR-1 mRNA was increased significantly in aged human cortical tissue from individuals that were not demented, which suggests that increased RyRs may have a protective or positive role to play in neuronal function. Furthermore, it has been shown recently that RyR-3 mRNA and protein levels are increased in the superior cervical ganglia of aged rats and may serve to protect neurons from oxidative stress by modulating and increasing the protein expression of neuronal nitric-oxide synthase (43). A clearer picture of how RyRs are involved in balancing normal and pathological aging is required before they can be considered a feasible therapeutic target.

Acknowledgments—We thank Dr. D. Westaway, University of Toronto, for the TgCRND8 mice and Dr. V. Sorrentino, University of Siena for the RyR antibodies.

REFERENCES

1. Kelliher, M., Fastbom, J., Cowburn, R. F., Bonkale, W., Ohm, T. G., Ravid, R., Sorrentino, V., and O'Neill, C. (1999) *Neuroscience* **92,** 499–513
2. Hardy, J., and Selkoe, D. J. (2002) *Science* **297,** 353–356
3. Selkoe, D. J. (2001) *Proc. Natl. Acad. Sci. U. S. A.* **98,** 11039–11041
4. LaFerla, F. M. (2002) *Nat. Rev. Neurosci.* **3,** 862–872
5. Ghosh, A., and Greenberg, M. E. (1995) *Science* **268,** 239–247
6. O'Neill, C., Cowburn, R. F., Bonkale, W. L., Ohm, T. G., Fastbom, J., Carmody, M., and Kelliher, M. (2001) *Biochem. Soc. Symp.* **67,** 177–194
7. Verkhratsky, A. (2002) *Cell Calcium* **32,** 393–404
8. Sorrentino, V., and Rizzuto, R. (2001) *Trends Pharmacol. Sci.* **22,** 459–464
9. Mattson, M. P., LaFerla, F. M., Chan, S. L., Leissring, M. A., Shepel, P. N., and Geiger, J. D. (2000) *Trends Neurosci.* **23,** 222–229
10. Chan, S. L., Mayne, M., Holden, C. P., Geiger, J. D., and Mattson, M. P. (2000) *J. Biol. Chem.* **275,** 18195–18200
11. Lee, S. Y., Hwang, D. Y., Kim, Y. K., Lee, J. W., Shin, I. C., Oh, K. W., Lee, M. K., Lim, J. S., Yoon do, Y., Hwang, S. J., and Hong, J. T. (2006) *FASEB J.* **20,** 151–153
12. Stutzmann, G. E., Smith, I., Caccamo, A., Oddo, S., Laferla, F. M., and Parker, I. (2006) *J. Neurosci.* **26,** 5180–5189
13. Smith, I. F., Hitt, B., Green, K. N., Oddo, S., and LaFerla, F. M. (2005) *J. Neurochem.* **94,** 1711–1718
14. Giannini, G., Conti, A., Mammarella, S., Scrobogna, M., and Sorrentino, V. (1995) *J. Cell Biol.* **128,** 893–904
15. Ogawa, Y. (1994) *Crit. Rev. Biochem. Mol. Biol.* **29,** 229–274
16. Chishti, M. A., Yang, D. S., Janus, C., Phinney, A. L., Horne, P., Pearson, J., Strome, R., Zuker, N., Loukides, J., French, J., Turner, S., Lozza, G., Grilli, M., Kunicki, S., Morissette, C., Paquette, J., Gervais, F., Bergeron, C., Fraser, P. E., Carlson, G. A., George-Hyslop, P. S., and Westaway, D. (2001) *J. Biol. Chem.* **276,** 21562–21570
17. Rossi, D., Simeoni, I., Micheli, M., Bootman, M., Lipp, P., Allen, P. D., and Sorrentino, V. (2002) *J. Cell Sci.* **115,** 2497–2504
18. Genazzani, A. A., Carafoli, E., and Guerini, D. (1999) *Proc. Natl. Acad. Sci. U. S. A.* **96,** 5797–5801
19. Jarvis, C. R., Lilge, L., Vipond, G. J., and Andrew, R. D. (1999) *Neuroimage* **10,** 357–372
20. Mattson, M. P., Gary, D. S., Chan, S. L., and Duan, W. (2001) *Biochem. Soc. Symp.* **67,** 151–162
21. Glazner, G. W., Chan, S. L., Lu, C., and Mattson, M. P. (2000) *J. Neurosci.* **20,** 3641–3649
22. Kim, H. S., Park, C. H., Cha, S. H., Lee, J. H., Lee, S., Kim, Y., Rah, J. C., Jeong, S. J., and Suh, Y. H. (2000) *FASEB J.* **14,** 1508–1517
23. Guo, Q., Fu, W., Sopher, B. L., Miller, M. W., Ware, C. B., Martin, G. M., and Mattson, M. P. (1999) *Nat. Med.* **5,** 101–106
24. Ye, C., Walsh, D. M., Selkoe, D. J., and Hartley, D. M. (2004) *Neurosci. Lett.* **366,** 320–325
25. Shmigol, A., Kirischuk, S., Kostyuk, P., and Verkhratsky, A. (1994) *Pfluegers Arch.* **426,** 174–176
26. Emptage, N., Bliss, T. V., and Fine, A. (1999) *Neuron* **22,** 115–124
27. Linn, C. L., and Gafka, A. C. (2001) *J. Physiol.* (*Lond.*) **535,** 47–63
28. Clodfelter, G. V., Porter, N. M., Landfield, P. W., and Thibault, O. (2002) *Eur. J. Pharmacol.* **447,** 189–200
29. Arundine, M., and Tymianski, M. (2003) *Cell Calcium* **34,** 325–337
30. Berridge, M. J. (2001) *Novartis Found. Symp.* **239,** 52–57, 150–159
31. Chui, D. H., Tanahashi, H., Ozawa, K., Ikeda, S., Checler, F., Ueda, O., Suzuki, H., Araki, W., Inoue, H., Shirotani, K., Takahashi, K., Gallyas, F., and Tabira, T. (1999) *Nat. Med.* **5,** 560–564
32. Hyde, L. A., Kazdoba, T. M., Grilli, M., Lozza, G., Brusa, R., Zhang, Q., Wong, G. T., McCool, M. F., Zhang, L., Parker, E. M., and Higgins, G. A. (2005) *Behav. Brain Res.* **160,** 344–355
33. Balschun, D., Wolfer, D. P., Bertocchini, F., Barone, V., Conti, A., Zuschratter, W., Missiaen, L., Lipp, H. P., Frey, J. U., and Sorrentino, V. (1999) *EMBO J.* **18,** 5264–5273
34. Futatsugi, A., Kato, K., Ogura, H., Li, S. T., Nagata, E., Kuwajima, G., Tanaka, K., Itohara, S., and Mikoshiba, K. (1999) *Neuron* **24,** 701–713
35. Reyes, M., and Stanton, P. K. (1996) *J. Neurosci.* **16,** 5951–5960
36. Nishiyama, M., Hong, K., Mikoshiba, K., Poo, M. M., and Kato, K. (2000) *Nature* **408,** 584–588
37. Unni, V. K., Zakharenko, S. S., Zablow, L., DeCostanzo, A. J., and Siegelbaum, S. A. (2004) *J. Neurosci.* **24,** 9612–9622
38. Bouchard, R., Pattarini, R., and Geiger, J. D. (2003) *Prog. Neurobiol.* **69,** 391–418
39. Rogawski, M. A., and Wenk, G. L. (2003) *CNS Drug Rev.* **9,** 275–308
40. Stutzmann, G. E. (2005) *Neuroscientist* **11,** 110–115
41. Mori, F., Okada, M., Tomiyama, M., Kaneko, S., and Wakabayashi, K. (2005) *Epilepsy Res.* **65,** 59–70
42. Lu, T., Pan, Y., Kao, S. Y., Li, C., Kohane, I., Chan, J., and Yankner, B. A. (2004) *Nature* **429,** 883–891
43. Vanterpool, C. K., Vanterpool, E. A., Pearce, W. J., and Buchholz, J. N. (2006) *J. Appl. Physiol.* **101,** 392–400